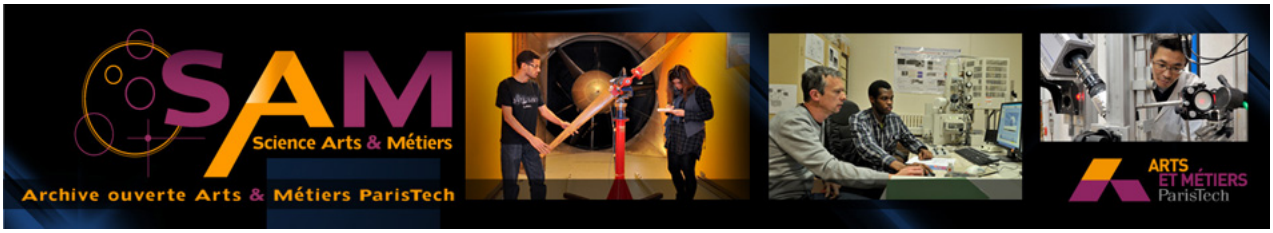

A comparative study of Forming Limit Diagrams predicted by two different plasticity theories involving vertex effects

Holanyo K. AKPAMA[1,a] , Mohamed BEN BETTAIEB[1,b*]

and Farid ABED-MERAIM[1,c]

[1]LEM3, UMR CNRS 7239 - Arts et Métiers ParisTech, 4 rue Augustin Fresnel, 57078 Metz Cedex 3, France

[a]holanyo.akpama@ensam.eu, [b]mohamed.benbettaieb@ensam.eu, [c]farid.abedmeraim@ensam.eu

Keywords: deformation theory of plasticity, crystal plasticity, Taylor scheme, Forming Limit Diagrams

Abstract. The main objective of this contribution is to compare the Forming Limit Diagrams (FLDs) predicted by the use of two different vertex theories. The first theory is micromechanical and is based on the use of the Schmid law, within the framework of crystal plasticity coupled with the Taylor scale-transition scheme. The second theory is phenomenological and is based on the deformation theory of plasticity. For both theories, the mechanical behavior is formulated in the finite strain framework and is assumed to be isotropic and rate-independent. The theoretical framework of these approaches will be presented in details. In the micro-macro modeling, the isotropy is ensured by considering an isotropic initial texture. In the phenomenological modeling, the material parameters are identified on the basis of micro-macro simulations of tensile tests.

Introduction

The determination of Forming Limit Diagrams (FLDs) through numerical modeling and simulations represents an interesting alternative to the experimental tests. Indeed, the relatively high costs along with the technical difficulties related to the experimental measurements motivate the manufacturers and scientists to turn to numerical modeling. To this end, several analytical and numerical criteria have been developed in the literature to predict the occurrence of localized necking and then to determine the FLDs. Among the commonly adopted approaches, one can quote the maximum force criterion introduced by Considère [1], the general bifurcation criterion initiated by Drucker [2] and Hill [3] and the initial imperfection approach proposed by Marciniak and Kuczynski [4]. In this paper the bifurcation criterion developed by Rice [5] is adopted to predict the FLDs. This choice is motivated by the sound mathematical foundations of this criterion. Furthermore, no fitting parameter is required for the application of this criterion, in contrast to, e.g., the initial imperfection parameter required by the Marciniak and Kuczynski approach. However, the application of the Rice bifurcation criterion requires the introduction of some destabilizing effects in the constitutive modeling in order to obtain realistic limit strains. These destabilizing effects may be due to some softening phenomena (induced by damage or temperature), or to the use of yield surfaces that develop a vertex-like structure during continued deformation. This latter choice is followed in this work. The consequence of such a vertex formation is a reduction in the instantaneous shear moduli, which allows predicting realistic limit strains [6]. Note that the development of such a destabilizing vertex may be due to the application of the deformation theory of plasticity (see, e.g., Stören and Rice [5], Hutchinson and Neale [5]), or to the use of crystal plasticity theory through the Schmid law of the single crystal coupled with scale-transition schemes (see, e.g., Yoshida and Kuroda [6], Gerald Franz et al. [7]). In this paper, the FLDs obtained by the deformation theory of plasticity are compared with those yielded by the crystal plasticity theory. The material parameters are selected in order to have the same uniaxial mechanical response with the two theories (the same stress-strain tensile curve).

Notations and conventions

In this paper, vector and tensor fields are underlined. Einstein's convention of summation over repeated indices is adopted. The range of the free (resp. dummy) index is indicated before (resp. after) the corresponding equation. The transpose of a tensor $\underline{X}$ is denoted by ${}^{T}\underline{X}$.

Micromechanical modeling

Modeling at the single crystal scale. The mechanical behavior of the single crystal is assumed to be rate-independent and is formulated in the finite strain framework. In this case, the constitutive modeling is defined by four equation families:

- The microscopic velocity gradient $\underline{g}$ is additively decomposed into its symmetric part $\underline{d}$ and its skew part $\underline{w}$. The tensor $\underline{d}$ (resp. $\underline{w}$) is itself decomposed into elastic strain rate part $\underline{d}^{e}$ (resp. lattice rotation rate $\underline{w}^{e}$) and plastic strain rate part $\underline{d}^{p}$ (resp. plastic spin $\underline{w}^{p}$):

$$\underline{d} = \frac{1}{2}\left(\underline{g} + {}^{T}\underline{g}\right) = \underline{d}^{e} + \underline{d}^{p} \quad ; \quad \underline{w} = \frac{1}{2}\left(\underline{g} - {}^{T}\underline{g}\right) = \underline{w}^{e} + \underline{w}^{p} \tag{1}$$

- The plastic deformation is solely due to the slip on the crystallographic slip systems:

$$\underline{d}^{p} = \frac{1}{2}\dot{\gamma}^{\alpha}(\underline{M}^{\alpha} + {}^{T}\underline{M}^{\alpha}) = \dot{\gamma}^{\alpha}\underline{R}^{\alpha} \quad ; \quad \underline{w}^{p} = \frac{1}{2}\dot{\gamma}^{\alpha}(\underline{M}^{\alpha} - {}^{T}\underline{M}^{\alpha}) = \dot{\gamma}^{\alpha}\underline{S}^{\alpha} \quad ; \quad \alpha = 1,...,2N_{s} \tag{2}$$

where $\dot{\gamma}^{\alpha}$ (resp. $\underline{M}^{\alpha}$) is the slip rate (resp. Schmid orientation tensor) for a given slip system α and N_{s} is the number of slip systems.

- The elastic behavior is defined by a hypo-elastic law and the plastic behavior obeys the Schmid law:

$$\begin{aligned} &\underline{C} : \underline{d}^{e} = \dot{\underline{\sigma}} - \underline{w}^{e}.\underline{\sigma} + \underline{\sigma}.\underline{w}^{e} \quad ; \quad \underline{w}^{e} = \dot{\underline{r}}.{}^{T}\underline{r} \\ &\forall \alpha = 1,...,2N_{s} \quad : \quad \tau^{\alpha} \le \tau_{c}^{\alpha} \quad ; \quad \dot{\gamma}^{\alpha} \ge 0 \quad ; \quad \left(\tau^{\alpha} - \tau_{c}^{\alpha}\right)\dot{\gamma}^{\alpha} = 0 \end{aligned} \tag{3}$$

where $\underline{C}$ is the isotropic elasticity matrix and $\underline{r}$ is the rotation of the crystallographic lattice. τ^{α} (resp. τ_{c}^{α}) denotes the resolved shear stress (resp. the critical shear stress) of slip system α. Their evolutions are defined by the following equations:

$$\forall \alpha = 1,...,2N_{s} \quad ; \quad \dot{\tau}^{\alpha} = \underline{R}^{\alpha} : (\dot{\underline{\sigma}} - \underline{w}^{e}.\underline{\sigma} + \underline{\sigma}.\underline{w}^{e}) \quad ; \quad \dot{\tau}_{c}^{\alpha} = H^{\alpha\beta}\dot{\gamma}^{\beta} \quad ; \quad \beta = 1,...,2N_{s} \tag{4}$$

where $\underline{H}$ is the hardening matrix.

- The nominal stress rate $\dot{\underline{n}}$ can be related to the Cauchy stress rate $\dot{\underline{\sigma}}$ by:

$$\dot{\underline{n}} = j\underline{f}^{-1}.(\dot{\underline{\sigma}} + \underline{\sigma}\,\mathrm{Tr}(\underline{d}) - \underline{g}.\underline{\sigma}) \tag{5}$$

where $\underline{f}$ is the deformation gradient, j its determinant, and Tr denotes the trace operator.

After some mathematical derivations of the consistency condition deduced from the Schmid law (3)$_{(2)}$, and using Eqs. (1), (2), (3)$_{(1)}$, (4), the slip rates of the active slip systems can be expressed as:

$$\forall g \in \mathcal{A} \quad ; \quad \left(\underline{R}^{g} : \underline{C} : \underline{R}^{h} + H^{gh}\right)\dot{\gamma}^{h} = \Psi^{gh}\dot{\gamma}^{h} = \underline{R}^{g} : \underline{C} : \underline{d} \quad ; \quad h \in \mathcal{A} \tag{6}$$

where $\mathcal{A}$ is the set of active slip systems.

Starting from relation (5) between $\dot{\underline{n}}$ and $\dot{\underline{\sigma}}$, and using the other constitutive equations (Eqs. (1), (2), (3)$_{(1)}$ and (4)), one can relate $\dot{\underline{n}}$ to $\underline{g}$ by the tangent modulus $\underline{\underline{l}}$

$$\dot{\underline{n}} = \underline{\underline{l}} : \underline{g} \tag{7}$$

The expression of $\underline{\underline{l}}$ is given as follows (see [7] for more details):

$$\underline{\underline{l}} = \left[\underline{\underline{C}} + {}_1\underline{\underline{l}} - {}_2\underline{\underline{l}} - {}_3\underline{\underline{l}} - \sum_{g,h \in \mathcal{A}} \left(\underline{\underline{C}} : \underline{\underline{R}}^g + \underline{\underline{S}}^g . \underline{\underline{\sigma}} - \underline{\underline{\sigma}} . \underline{\underline{S}}^g \right) M^{gh} \underline{\underline{R}}^h : \underline{\underline{C}} \right] \tag{8}$$

where:

$$\forall\, i,j,k,l = 1,2,3 : \quad {}_1l_{ijkl} = \sigma_{ij}\delta_{kl} \quad ; \quad {}_2l_{ijkl} = \frac{1}{2}\left(\delta_{lj}\sigma_{ik} - \delta_{kj}\sigma_{il} \right) \quad ; \quad {}_3l_{ijkl} = \frac{1}{2}\left(\delta_{ki}\sigma_{lj} - \delta_{li}\sigma_{kj} \right) \tag{9}$$

and $\underline{\underline{M}}$ is the inverse of $\underline{\underline{\Psi}}$.

An explicit/implicit algorithm has been developed by Akpama et al. in [9] in order to incrementally integrate the constitutive equations at the single crystal scale and then to compute the tangent modulus $\underline{\underline{l}}$.

Modeling at the polycrystal scale. The mechanical behavior of the polycrystal is derived from that of the individual single crystals using the Taylor scale-transition scheme. With this transition scheme, the deformation is assumed to be homogeneous over the polycrystal. Therefore, the macroscopic velocity gradient $\underline{\underline{G}}$ is equal to its microscopic counterpart $\underline{\underline{g}}$. This choice implies that the macroscopic tangent modulus $\underline{\underline{\mathscr{L}}}$, relating the macroscopic stress rate $\dot{\underline{\underline{N}}}$ to $\underline{\underline{G}}$, can be deduced from its microscopic counterpart $\underline{\underline{l}}$ by the following basic averaging rule over the representative volume element V of the polycrystal:

$$\underline{\underline{\mathscr{L}}} = \frac{1}{V} \int_V \underline{\underline{l}} \, dV \tag{10}$$

Plane stress condition. The studied sheets are assumed to be thin. Accordingly, the bifurcation analysis can be carried out under the following plane-stress conditions:

$$\dot{N}_{i3} = 0 \text{ and } \dot{N}_{3i} = 0 \tag{11}$$

This latter condition permits (after some lengthy but straightforward calculations) to derive the in-plane macroscopic tangent modulus $\underline{\underline{\mathscr{L}}}^{PS}$ from $\underline{\underline{\mathscr{L}}}$.

Phenomenological modeling

The deformation theory is used in this phenomenological part to model the mechanical behavior of the studied metal sheets. In this modeling, the material is assumed to be isotropic, incompressible and strain-rate independent. The tangent modulus $\underline{\underline{\mathscr{L}}}^{PS}$ determined under the plane-stress condition has been derived by Hutchinson and Neale [5]. For the sake of brevity, the expression of this modulus is introduced in this work without detailing the related mathematical developments (interested readers may refer to [5]). The Jaumann derivative of the in-plane Cauchy stress tensor ${}^J\underline{\underline{\Sigma}}^{PS}$ is related to the in-plane strain rate tensor $\underline{\underline{D}}^{PS}$ (symmetric part of the in-plane velocity gradient $\underline{\underline{G}}^{PS}$) by the instantaneous modulus $\underline{\underline{L}}^{PS}$:

$${}^J\underline{\underline{\Sigma}}^{PS} = \underline{\underline{L}}^{PS} : \underline{\underline{D}}^{PS} \tag{12}$$

Only the components L^{PS}_{1111}, L^{PS}_{2222}, L^{PS}_{1122}, L^{PS}_{2211}, and L^{PS}_{1212} are different from zero and are defined by the following expressions:

$$L^{PS}_{1111} = \frac{4}{3}E_s - (E_s - E_t)(\Sigma_{11}/\Sigma_e)^2 \quad ; \quad L^{PS}_{2222} = \frac{4}{3}E_s - (E_s - E_t)(\Sigma_{22}/\Sigma_e)^2$$
$$L^{PS}_{1122} = L^{PS}_{2211} = \frac{2}{3}E_s - (E_s - E_t)((\Sigma_{11}\Sigma_{22})/\Sigma_e^2) \quad ; \quad L^{PS}_{1212} = \frac{1}{3}E_s(\varepsilon_{11} - \varepsilon_{22})\frac{e^{2\varepsilon_{11}} + e^{2\varepsilon_{22}}}{e^{2\varepsilon_{11}} - e^{2\varepsilon_{22}}} \tag{13}$$

where Σ_e is the von Mises equivalent stress. E_s and E_t are the secant modulus and tangent modulus of the uniaxial true stress-Eulerian strain curve at Σ_e. In this work, the Hollomon hardening law $(\Sigma_e = K\varepsilon_e^n)$ is used. In this case, the secant and tangent moduli are given by:

$$E_s = K\varepsilon_e^{N-1} \quad ; \quad E_t = NK\varepsilon_e^{N-1} \tag{14}$$

The in-plane nominal stress rate $\dot{\underline{N}}^{PS}$ is related to the in-plane velocity gradient $\underline{G}^{PS}$ by:

$$\dot{\underline{N}}^{PS} = \underline{\mathscr{L}}^{PS} : \underline{G}^{PS} \tag{15}$$

where the tangent modulus $\underline{\mathscr{L}}^{PS}$ is related to the instantaneous modulus $\underline{L}^{PS}$ by:

$$\underline{\mathscr{L}}^{PS} = \underline{L}^{PS} - {}_1\underline{L} - {}_2\underline{L} \tag{16}$$

Tensors ${}_1\underline{L}$ and ${}_2\underline{L}$ are given by the following index expressions:

$$\forall i,j,k,l = 1,2: \quad {}_1L_{ijkl} = \frac{1}{2}[\delta_{ik}\Sigma_{lj} + \delta_{il}\Sigma_{kj}] \quad ; \quad {}_2L_{ijkl} = \frac{1}{2}[\Sigma_{ik}\delta_{lj} - \Sigma_{il}\delta_{jk}] \tag{17}$$

Rice bifurcation criterion

The strain localization is considered as a bifurcation from the material response. This bifurcation is searched for as a localization band, which is determined by its normal unit vector $\vec{N}$ and which represents the non-homogeneity in the velocity gradient. ${}^{+}\underline{G}^{PS}$ and ${}^{-}\underline{G}^{PS}$ designate, respectively, the in-plane velocity gradient inside and outside the band. Maxwell's compatibility condition, for the velocity field, states that there exists a vector $\dot{\vec{C}}$ such that the jump in $\underline{G}^{PS}$ through the band reads:

$$[\![\underline{G}^{PS}]\!] = {}^{+}\underline{G}^{PS} - {}^{-}\underline{G}^{PS} = \dot{\vec{C}} \otimes \vec{N} \tag{18}$$

On the other hand, the equilibrium condition implies the continuity of the nominal stress rate vector across the band:

$$\vec{N}.[\![\dot{\underline{N}}^{PS}]\!] = \vec{N}.\left({}^{+}\dot{\underline{N}}^{PS} - {}^{-}\dot{\underline{N}}^{PS}\right) = \vec{0} \tag{19}$$

By introducing the behavior law $\dot{\underline{N}}^{PS} = \underline{\mathscr{L}}^{PS} : \underline{G}^{PS}$ in Eq. (19), and using Eq. (18), one finally obtains (see [7]):

$$(N_i \mathscr{L}^{PS}_{ijkl} N_l)\dot{C}_k = 0 \Leftrightarrow (\vec{N}.\underline{\mathscr{L}}^{PS}.\vec{N}).\dot{\vec{C}} = \vec{0} \tag{20}$$

From Eq. (20), two families of solutions can be extracted. The first possibility is when $\dot{\vec{C}}$ is a null vector, and thus the magnitude of the jump is zero, in which case there is no bifurcation. The second possibility corresponds to the existence of at least one non-zero $\dot{\vec{C}}$, in which case the system of Eq. (20) has an infinite number of solutions leading to the following condition:

$$\det(\vec{N}.\underline{\mathscr{L}}^{PS}.\vec{N}) = 0 \tag{21}$$

Eq. (21) is the so-called Rice's criterion ([5]) corresponding to the loss of ellipticity of the boundary value problem. From Eq. (21), the loss of ductility is considered to be reached when the first zero eigenvalue is seen in the acoustic tensor.

Numerical results

In this part, a polycrystal made of 1000 BCC single crystals is considered. The hardening law of the single crystals is the same as that used in [7]. An isotropic initial texture is generated by a random distribution of quaternions [12]. In order to assess the isotropy of the mechanical response of the polycrystal, 10 tensile tests in the plane of the sheet are simulated. Only the tensile direction is varied from one test to another. The angle θ between the tensile direction and the rolling direction is varied from 0° to 90° at intervals of 10°. In Fig. 1(a), the tensile stress–strain curves are plotted for the different tensile orientations. The different curves are indistinguishable, which gives a first indication of the isotropy of the polycrystal. In Fig. 1(b), the evolution of the Lankford coefficient as a function of the tensile direction θ is plotted. This coefficient is comprised between 0.7 and 0.9, which demonstrates the slight anisotropy of the studied polycrystal. Therefore, it is reasonable to assume that the behavior of the polycrystal is isotropic. The parameters of the Hollomon isotropic hardening law, used when the deformation theory is applied, are fitted on the basis of the tensile tests of Fig. 1(a). After fitting, K and N seem to be equal to 1761 MPa and 0.335, respectively. These parameters are then employed to compute the tangent modulus of Eq. (16) and then to predict the ductility limits. With this choice, the uniaxial mechanical response becomes the same for the two different theories of plasticity. The difference between the FLDs predicted by the application of the Taylor scheme and the deformation theory is displayed in Fig. 1(c). It is worth noting that the predicted limit strain for the uniaxial tensile path is the same for both theories. Fig. 1(c) demonstrates that the two FLDs determined by the two theories of plasticity are quite different in the whole, especially in the right-hand side of the FLD. This reveals, as expected, that the perfect similarity in terms of uniaxial mechanical response is far not sufficient to provide comparable limit strains. The interpretation of this result becomes obvious when considering that the bifurcation criterion is essentially related to the evolution of the tangent modulus, which involves not only the stress state itself, but also the stress derivatives.

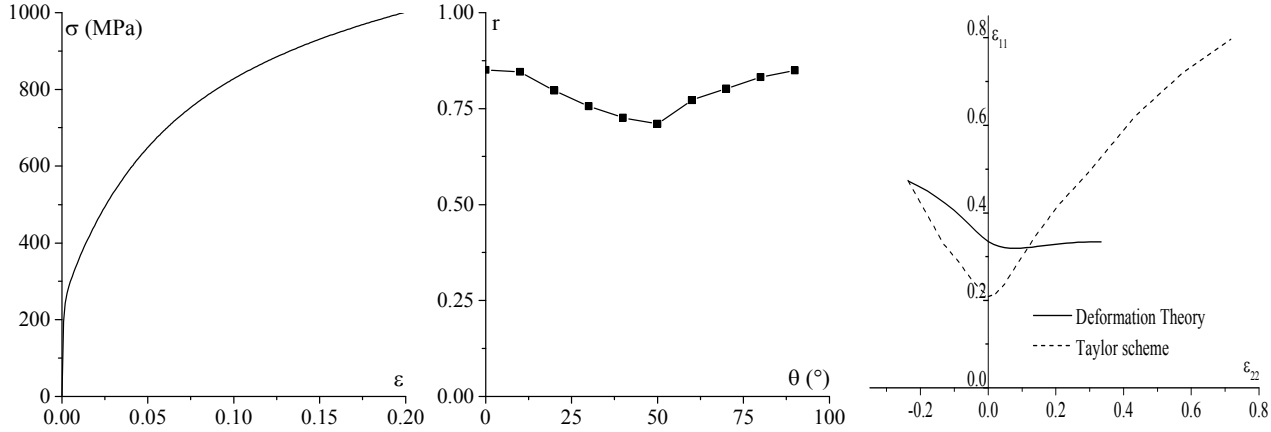

Fig. 1. Numerical results: (a) Tensile stress–strain curves of the polycrystal for the different tensile orientations, (b) Evolution of the Lankford coefficient of the polycrystal as a function of the tensile direction θ, (c) Comparison between the FLD predicted by the deformation theory and the FLD predicted by the Taylor scale-transition scheme in the context of crystal plasticity.

Conclusions

In this paper, two different plasticity theories involving vertex effects have been detailed and combined with the Rice bifurcation criterion to predict the ductility limits in the form of FLDs. To

be consistent with the planar Rice criterion, the tangent moduli for both theories have been expressed in the plane of the sheet, thus satisfying the plane-stress condition. The numerical results demonstrate a large difference between the FLDs predicted by the two theories, although the uniaxial mechanical response is the same. This work will be improved in the future by taking into account the effect of plastic anisotropy in the comparisons between the predictions of the two theories.

References

[1] A. Considère, Mémoire sur l'emploi du fer et de l'acier dans les constructions, Ann. Ponts et Chausées. 9 (1885), 574-775.

[2] D.C. Drucker, Some implications of work hardening and ideal plasticity, Q. Appl. Math. 7 (1950), 411-418.

[3] R. Hill, A general theory of uniqueness and stability in elastic-plastic solids, J. Mech. Phys. Solids. 6 (1958), 239-249.

[4] Z. Marciniak, K. Kuczynski, Limit strains in processes of stretch-forming sheet metal, Int. J. Mech. Sci. 9 (1967), 609-620.

[5] S. Stören, J.R. Rice, Localized necking in thin sheets, J. Mech. Phys. Solids 23 (1975), 421-441.

[6] M. Ben Bettaieb, F. Abed-Meraim, Investigation of localized necking in substrate-supported metal layers: Comparison of bifurcation and imperfection analyses, International Journal of Plasticity 65 (2015), 168-190.

[5] J.W. Hutchinson, K.W. Neale, Sheet necking – II. Time-independent behavior. In: Koistinen, D.P., Wang, N.M. (Eds.), Mechanics of Sheet Metal Forming. Plenum, 1978, pp. 127-153.

[6] K. Yoshida, M. Kuroda, Numerical investigation on a key factor in superior stretchability of face-centered cubic polycrystalline sheets, Int. J. Mech. Sci., 58 (2012), 47-56.

[7] G. Franz, F. Abed-Meraim, M. Berveiller, Strain localization analysis for single crystals and polycrystals: Towards microstructure–ductility linkage, International Journal of Plasticity 48 (2013), 1-33.

[8] J.W. Hutchinson, V. Tvergaard, Shear band formation in plane-strain, Int. J. Solids Struct., 17 (1981), 451-470.

[9] H.K. Akpama, M. Ben Bettaieb, F. Abed-Meraim, Numerical integration of rate-independent BCC single crystal plasticity models: comparative study of two classes of numerical algorithms, submitted to Comput. Meth. Appl. Mech. Eng.

[12] C. Miehe, J. Schröder, J. Schotte, 1999. Computational homogenization analysis in finite plasticity. Simulation of texture development in polycrystalline materials. Comput. Meth. Appl. Mech. Eng. 171, 387-418.